Developments of a thick and large solid hydrogen target for radioisotope beams

T.Moriguchi[a], S.Ishimoto[b], S.Igarashi[a], A.Ozawa[a], Y.Abe[a], Y.Ishibashi[a], Y.Ito[a], H.Ooishi[a], H.Suzuki[a], M.Takechi[c], K.Tanaka[c],

a Institute of Physics, University of Tsukuba, Tsukuba, Ibaraki 305-8571, Japan

b High Energy Accelerator Research Organization (KEK), Tsukuba, Ibaraki 305-0801, Japan

c RIKEN Nishina Center, Wako, Saitama 351-0198, Japan

Abstract

A thick and large solid hydrogen target (SHT) for radioisotope (RI) beams was developed. A target with 100 mm thickness and 50 mm diameter equipped with thin Kapton windows (25 μm) was achieved. We developed a new method to fill solid hydrogen into a large target cell by eliminating any void or porous regions. The expansion of thin Kapton windows and the real thickness of SHT were measured by a laser distance meter and an energy-loss of RI beams, respectively. They gave the same thickness confirming the complete solidification of hydrogen in the cell. We obtained a window expansion of about 2.5 mm (about 1.25 mm for each side).

Keywords: Solid hydrogen target; RI-beam

1. Introduction

The proton is used as a probe to explore the internal structure of nucleus in nuclear physics experiments. From an experimental point of view, a liquid and/or solid hydrogen target is very attractive for radioisotope (RI) beam experiments. Since the number of atoms per unit mass is the maximum in the targets compared to other heavier targets, the small intensity of RI beams can be partly compensated. Multiple scattering effects of RI beams inside the target are also very small in the liquid and solid hydrogen target. In RIKEN, liquid hydrogen targets have been developed as a consequence [1].

Among RI-beam experiments, measurements of the reaction cross sections (σ_R) are one of the most sensitive measurements. We can have a good experimental accuracy (a few %), even for a very low beam-intensity (~0.1 cps) in these

measurements. Although a carbon target has usually been used due to easy handling, a hydrogen target is also very attractive in the measurements. Recently, σ_R of the drip-line nucleus ^{22}C has been measured using a liquid-hydrogen target [2]. For RI beams with high energies (~ a few 100 *A* MeV), a thick hydrogen target (~100 mm) is required. Furthermore, since the size of the RI-beam is fairly large (typically, a few cm diameter), a large-size target is also necessary. From an experimental point of view, a solid hydrogen target (SHT) has advantages compared with a liquid one:

1) The density is large by about 20%.

2) No temperature control is needed for a stable operation. Temperature control is necessary for the liquid target to keep the same density.

3) A thin window is available since the operating pressure is much lower than the liquid target. Furthermore, a windowless target is possible.

Previously, we developed a windowless SHT for proton elastic-scattering experiments with RI beams [3]. This time, we adopted the same technique to make SHT with much more thickness and larger size.

In this paper we present the new SHT system. The method of fabrication is given in section 2. In section 3, we describe the measurements of thickness and their results. Finally, we give a summary in section 4.

2. Thick and large solid hydrogen target

Fig. 2-1 and 2-2 show the target cell of SHT. The target cell consists of three hollowed copper blocks joined into a single square pillar. A cylinder was hollowed out of blocks with a diameter of SHT. The diameter was 50 mm in the present SHT. The center block was a 18 mm thick rectangular block with a deep U-shaped cut on its long side. Its cross section was larger than those of two square side blocks. The target cell was attached to the cold head of a refrigerator by the U-shaped arms of the center block, which served good mechanical and thermal contacts. Since the cell was hung in high vacuum exposed to the radiation coming through windows of the target cryostat, the present cell structure was very helpful to provide a uniform and stable temperature. Three copper blocks were joined together with indium seals. Indium wires of 1.0 mm in diameter were used.

The thickness of SHT was changed, replacing a pair of side blocks to those of suitable thickness. We fabricated and used two SHT in beam experiments. They were 30 mm and 100 mm thickness. The 100 mm thickness SHT corresponds to the hydrogen thickness about 0.85 g/cm^2. Both ends of the cell were windows for incoming and outgoing particles. They were made of Kapton films with 25 μm thickness. Kapton films were glued on copper flames using an epoxy adhesive; Stycast 1266 A/B. The copper flames bolted the target cell on the outside. Two thin stainless steal pipes were connected to the center cell for supply and recovery of hydrogen gas.

The state of solid hydrogen must be constant all over in SHT for long periods of the experiments. Thus, the operating temperature must be kept sufficiently lower than the solidification temperature (15 K). We set it at about 4K, and used a G-M cryocooler, Sumitomo RDK-415D, which had a cooling power of 1.5 W at 4.2 K. The target and cold head temperatures were measured by Pt-Co resistance thermometers, Chino R800-6. A heater, Lakeshore HTR-25-100, was put near to the cold head to control the target temperature. Hydrogen gas was introduced into the cell through a 1/8"-tube of stainless steal at room temperature, as shown in Fig. 2-1. The inlet tube was connected to the top of the target cell. The hydrogen entrance was carefully designed using double-wall structure to reduce the heat conductance between the cell and the inlet tube. This structure prevented the inlet from being blocked by solidified hydrogen. This is important, as discussed in a later section.

Fig. 2-2 is a photo of a target cell of 100 mm thick cell and the cryocooler cold head. A 1/4" stainless-steal flexible tube was connected onto the top for the recovery of hydrogen gas. In principle, we had no need to recover hydrogen gas in the steady operation of SHT, because the temperature was so low that little evaporating gas escaped from the cell. Its purpose was mainly for safety and for the recovery of hydrogen after the experiment had been finished.

Fig. 2-3 shows a schematic view of the hydrogen handling system and the cryostat for SHT. Hydrogen gas was supplied from a 300-liter tank at room temperature. The supply pressure, P_{IN}, was controlled by an electrical valve, MKS 0248A-05000SV, with a controller 250E-1-D and Baratron 627B13TBC2B. The SHT cell was surrounded by a thermal radiation shield made of thin copper plates

in a vacuum chamber (pressure ~10^{-6} mbar). It took about 4 hours to reach around 4 K after the cryocooler started to work.

The key point of the method is that we have to keep the hydrogen inlet path open until the solidification of hydrogen was completed in the cell. If the path was blocked before the solidification was completed, voids remained in the solid. This was due to about 12% shrinkage of hydrogen when the liquid phase changed to the solid phase. Therefore, it was necessary to continue supplying hydrogen gas into the target cell until the solidification was completed in order to compensate for the shrinkage. The actual phenomena during solidification are complicated and described in detail in Ref. [4].

In the initial stage of development at KEK, we encountered the problem of voids produced along the center axis of the cell. This problem was solved by increasing the hydrogen flow rate by increasing the supplying pressure of hydrogen gas.

We used normal hydrogen, and changed the supply pressure, P_{IN}, between 50 mbar and 200 mbar (pressures measured at room temperature). Hydrogen gas was solidified without any transition to the liquid phase when P_{IN} was below 100 mbar. Taking into account the pressure drop, it was the gas-solid phase transition below the triple point of hydrogen, of which the temperature and pressure were 13.8 K and 70.4 mbar, respectively, in equilibrium, but 13.96 K and 72.0 mbar in normal hydrogen. In this case, large voids remained somewhere on the central axis. In Fig. 2-4 we show such voids produced at 67 mbar. We must notice that hydrogen was not in thermal equilibrium. The region near the inlet was warmest, so temperature gradients were produced from the cold wall toward the center in the cell and from both side blocks to the central block. The voids were produced by inhomogeneous solidification inside the cell as well as by shrinkage.

The liquid phase appeared, when P_{IN} exceeded 100 mbar. After liquefaction started, a solid was grown rapidly on the bottom side, so that liquid was as if it was in a cylinder of a transparent solid when observed through the windows. It showed the temperature gradients from the side wall to the central part and from the bottom to the top in the copper blocks produced by the warm gas flow from the top of the central block. The liquid level gradually rose as the temperature decreased. When P_{IN} was set at a high pressure, the cell temperature temporarily

rose before the solidification was completed. The solid was partially melted on the upper side, and the resultant liquid filled the voids. This may be attributed to melting of the upper thin solid, which partially blocked the gas flow inside the cell, due to a local increase of the gas pressure. Then, the cell temperature again decreased, and gradually reduced the gas-phase volume in a small region just below the inlet.

When P_{IN} was increased to 133 mbar, the gas phase disappeared from the cell before all hydrogen inside the cell was solidified. Solid without a void was successfully made. A typical solidification process at 133 mbar is shown in Fig. 2-5. In Fig. 2-5-(2) and 2-5-(3), we can see the changing liquid levels. After solidification was completed, the cell temperature again started to decrease, and finally reached about 4 K. However, the solid cracked near the inlet as the temperature decreased. The amount of cracks increased with pressure. A large temperature gradient was produced near the inlet by increasing the gas flow rate at low temperature. With P_{IN} being higher than 133 mbar, no void was observed. We optimized P_{IN} under the conditions of no-void and little cracks. The operating pressure was set at 133 mbar in our present system. SHT with an 100 mm thickness was completed in 2.5 hours after the gas filling started, as shown in Fig. 2-6. On the other hand, SHT with a 30 mm thickness was completed in 75 minutes. The dark parts on the top of the figure are cracks produced in the final cooling stage.

The solid in the cell was melted by the main heater located at the top of the cell. Hydrogen gas was recovered to the 300-liter tank (see Fig. 2-3). At the beginning of this recovery process, we also used a silicon rubber heater wrapped on a flexible tube in order to prevent any possible blocking near the inlet. The total time for recovery was about 30 minutes.

3. Measurements of thickness of SHT

When hydrogen gas is fulfilled in the cell, the Kapton windows swell due to an inner pressure. The real thickness of SHT depends on the curvature of the Kapton windows. Furthermore, the real thickness of the SHT depends on the homogeneity of the density of solid hydrogen. Therefore, we measured the thickness of SHT by using a laser distance meter and the energy-loss (ΔE) of RI

beams. The measurements by the laser distance meter are sensitive only to the curvature of the windows. On the other hand, since RI beams penetrate SHT, ΔE of RI beams depend on the real thickness of SHT. If there is any deterioration, such as voids and/or large porous regions, in the solid hydrogen, measurements by ΔE of RI beams will give inconsistent results with those by the laser distance meter. In these measurements, we used an SHT cell with a 30 mm thickness. The geometries of this SHT cell are shown in Fig. 3-1.

First, we describe measurements by the laser distance meter, Keyence LK500. We scanned the laser light in two directions on the SHT cell: a horizontal direction (X) and a vertical direction (Y), as shown in Fig. 3-1. Since the vacuum chamber has a window made of acryl, the laser light penetrated the acryl window before reaching the SHT cell. However, we checked that the reflection from the acryl window was sufficiently small. We painted the surface of the Kapton windows black so as to reflect the laser light efficiently. A typical result for scanning in the horizontal direction (X) across the center of the Kapton window is shown in Fig. 3-2, where a swollen front surface is shown between 17 and 67 mm on the X-axis. It is noted that the observed distance was corrected so that laser light scanning would be parallel to the surface of the center block of the SHT cell. The cross sections of the center copper block and the copper flame are also visible below 17mm and above 67 mm (0-17 and 67-84 mm) in Fig. 3-2. In Fig. 3-2, the coordinates Z = 0 mm and X = 0 mm correspond to the surface and the edge of the center block, respectively. Data points for the Kapton window area (17-67 mm in Fig. 3-2) were fitted by a second-order polynomial function. The result is also shown in Fig. 3-2. The expansion of a Kapton window is given by the difference of Z at the center (X=42 mm) and the edge (X=17 mm or 67 mm). We measured the expansion for both ends of the SHT cell. To check the reproducibility, we repeated the process of melt and solidification 4 times, and measured the expansion of both Kapton windows each time. The results are summarized in Fig. 3-3. It should be noted that we took only fitting errors (1-σ) into account for the errors of measurements. According to Fig. 3-3, all results agree within error bars. This consistency shows that the expansion of the Kapton windows were well reproducible in the present fabrication of SHT. We also measured the expansion in the vertical direction (Y direction in Fig. 3-1). For the vertical direction, we

measured the window expansion only once. By summing the window expansion of both ends, we obtained the 'total' expansion of SHT, as shown in Fig. 3-4. The results for both directions (X and Y) agree within error bars. Thus, averaging the data in both directions, as shown in Fig. 3-4, we obtained 2.55±0.26 mm for the expansion of windows measured by the laser distance meter.

Next, we measured the thickness of SHT utilizing RI beams. We measured the energy-loss (ΔE) of RI beams in the SHT and calculated the thickness from an energy-loss formula. The experimental setup for the measurement is shown in Fig. 3-5. An ^{11}Li beam produced in the RIPS facility in RIBF, RIKEN [5], was irradiated to SHT. The beam energy of ^{11}Li was ~45 *A* MeV. Typical count rate of the ^{11}Li beam was about 800 cps. We measured ΔE by two Si Solid State Detectors (SSD1 and SSD2) located downstream of SHT. Each SSD had an effective area of 100×100 mm^2 effective area with 0.1 mm thickness. The beam position in SHT was measured by two Parallel Plate Avalanche Counters (PPAC) located upstream of SHT. PPAC is charge division type [6] with an 100×100 mm^2 effective area. The typical beam envelope at SHT is shown in Fig. 3-6. In the figure, 0 mm means the center of the beam axis. We made position gates from -25 mm to +25 mm with a 2.5 mm step for the X and Y directions as shown in Fig. 3-6. A conversion from ΔE to the thickness of SHT was carried out by using the energy-loss formula in LISE++ [7]. The thickness in the horizontal direction (X) was deduced from ΔE in SSD1. The result is shown in Fig. 3-7. Since the thickness across the effective area of SSD may not be homogeneous, it had to be checked. We measured ΔE without solid hydrogen in the cell, but with Kapton windows, using SSD1, and deduced the thickness. The result is also given in Fig. 3-7. Subtracting the deduced thickness without solid hydrogen from that with solid hydrogen, the 'real' SHT thickness was obtained, which is shown in Fig. 3-8. The data points in Fig. 3-8 were fitted by a second-order polynomial function, as shown in Fig. 3-8 by a solid line. The expansion of Kapton window is given by the difference of the thickness between the fitted value at the center (X = 0 mm in Fig. 3-8) and those at the edges of the cell (X = ±25 mm in Fig. 3-8). We also obtained the expansion in the vertical direction (Y) in the same manner. We took an average of the results for the two directions. We also performed the same analysis for another SSD (SSD2). The results of the expansion of Kapton

windows deduced form ΔE of RI beams are summarized in Fig. 3-9. It is noted that we took only fitting errors (1-σ) into account for the errors. The results from SSD1 and SSD2 are very consistent each other. Averaging the two data, we obtained 2.40±0.63 mm as shown in Fig. 3-9. In Fig. 3-9, we also compare the result with that measured by the laser distance meter, where we took the averaged value in Fig. 3-4. The two results are very consistent, although the result measured by the laser distance meter is more accurate than that deduced from ΔE of RI beams. This consistency shows that there is no large deterioration inside SHT: such as voids, large porous regions, melting solid and so on, during the beam experiment. We also conclude that the expansion of the Kapton windows with 25 μm thickness was 2.5 mm at the center of the SHT cell with the diameter of 50 mm. This window expansion will be taken into account for in the present and future RI beam experiments with SHT.

4. Summary

We developed a thick and large solid hydrogen target (SHT) for radioisotope (RI) beam experiments. We succeeded to make an SHT with 100 mm thickness and 50 mm in diameter equipped with thin Kapton windows (25 μm). We found an optimum condition for the pressure to make SHT without any voids (133 mbar). We measured the expansion of windows, which can not be avoided in SHT with thin windows, by a laser distance meter and a measurement of the energy-loss of RI beams inside SHT. The thicknesses of SHT measured by the two methods give a consistent result. We obtained a window expansion of about 2.5 mm (about 1.25 mm for each side). This consistency shows that there is no large deterioration, such as voids, large porous regions, melting solid and so on, during the beam experiment. This large and thick SHT has already been used for two experiments with RI beams. We will also perform further measurements of reaction cross sections for unstable nuclei with this SHT.

This large and thick SHT could be used in nuclear physics experiments, such as high or medium-energy experiments at J-PARC and other fields. The method described here has no serious limit to enlarge the diameter and thickness of SHT, if we could avoid blocking at the inlet of a target sell. We point out a para-hydrogen target, which may improve the difficulties in fabrication of a large

target. The para-hydrogen has about a 300-times higher thermal conductivity than normal hydrogen at 4 K.

Acknowledgements

The authors gratefully acknowledge Prof. K. Morimoto for useful discussions and suggestions. The authors also gratefully acknowledge all staff members at the RIKEN ring cyclotron and RIPS facility for their stable operation of the RI beams. One of the authors (T.M.) is grateful for support from the Junior Research Associate program in RIKEN. The present work is partly supported by the Ministry of Education, Culture, Sports, Science and Technology through a Grant-In-Aid for Scientific Research under program number 18340074.

References

[1] H. Ryuto et al., Nucl. Instrum. Methods **A 555**, (2005) 1.

[2] K. Tanaka et al., Phys. Rev. Lett. **104**, (2010) 062701.

[3] S. Ishimoto et al., Nucl. Instrum. Methods **A 480**, (2002) 304.

[4] S. Ishimoto et al., Phys. Lett. **A 299**, (2002) 622.

[5] T. Kubo et al., Nucl. Instrum. Methods **B 70**, (1992) 309.

[6] H. Kumagai, K. Yoshida, RIKEN Accel. Prog. Rep. **28,** (1995) 127.

[7] O.B. Tarasov, D. Bazin, Nucl. Instrum. Methods **B 266**, (2008) 4657.

Figures

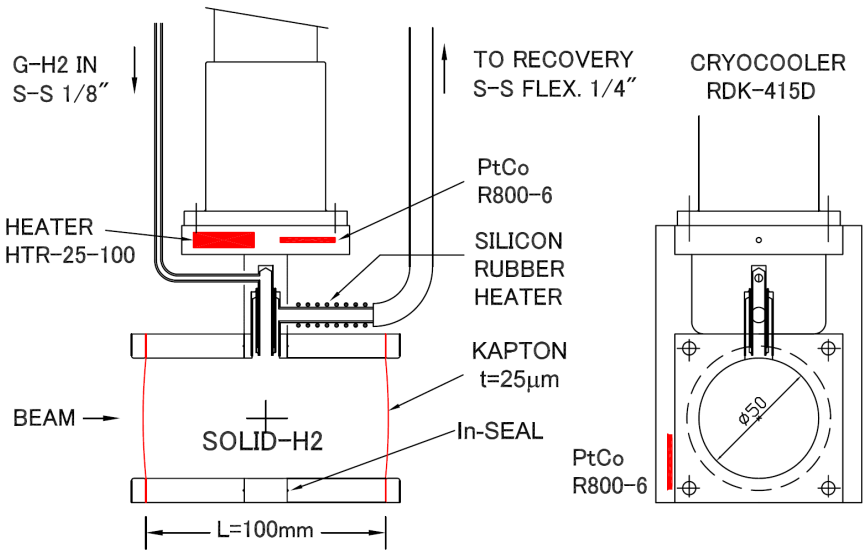

Fig. 2-1 Schematic view of a SHT cell with 100 mm thickness. Left and right figures are the side and front views of SHT, respectively. The target cell consists of three hollowed copper blocks joined into a single square pillar. The center copper block is hung from the cold head of the cryocooler. Both ends of the cell are made of thin Kapton films. The beam passes SHT along the symmetry axis in the horizontal direction. In the left figure, a thin hydrogen gas inlet tube is on the left and a thicker gas-recovery tube on the right. A double wall structure at the entrance of the cell prevents the tubes from blocking due to solidification of hydrogen. A Pt-Co thermometer is put inside the upper flange of the cell. A heater is set in the same flange for melting the solid. A silicon rubber heater is wrapped around the gas recovery tube.

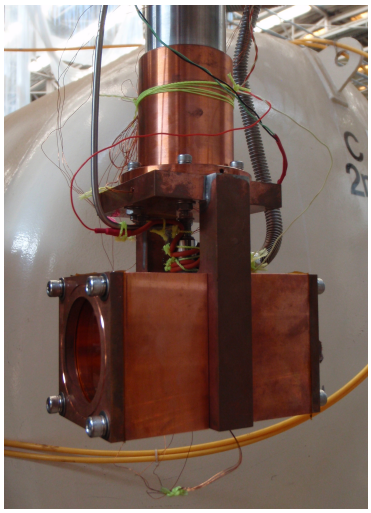

Fig. 2-2 Photo of a target cell with 100 mm thickness and the cryocooler cold head. A sidelong view of the target cell is given here. All parts are made of pure copper. The Kapton window and its fixing frame are in the front. The cell is hung from the cold head of the cryocooler by the U-shaped arms of the center block, making an excellent thermal contact. The hydrogen gas inlet and recovery tubes are seen on both sides.

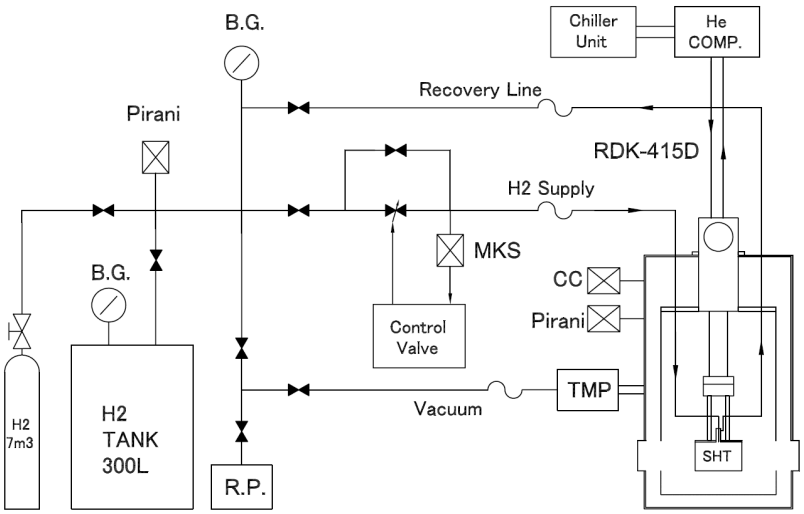

Fig. 2-3 Diagram of a hydrogen gas handling system. SHT is supported in high vacuum inside a target cryostat that has two windows for incoming and outgoing particles. He gas is supplied from a 300-liter tank at room temperature under the controlled pressure. The cryocooler RDK-5415D cools first the target cell to about 15 K, where hydrogen is solidified, and then to 4 K, the working temperature of SHT.

Fig. 2-4 Solid hydrogen by a pressure of 67 mbar. When hydrogen was solidified at low pressure (hydrogen supply pressure below 100 mbar), a large void was remained.

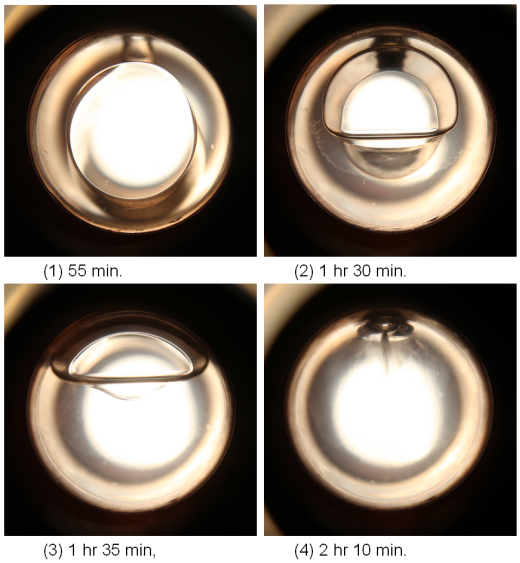

Fig. 2-5 Solid-hydrogen growth at the supply pressure of 133 mbar. The indicated times are those after the gas filling started. (1) Hydrogen is still in the gas phase. (2) Hydrogen is liquefied in the lower part of the cell. The upper half is occupied by the gas phase. (3) Liquid level is going up inside the hydrogen solid that is simultaneously growing from the side wall (not clearly seen in the photo). The dent in the inner part of the liquid level is made by blowing of the inlet gas. (4) Hydrogen just before solidification was completed. The gas phase occupies only a small volume below the gas inlet. Hydrogen solid occupies a large volume of the cell with a small amount of the liquid phase confined in it. Soon the gas phase was pushed out and liquid phase was completely solidified.

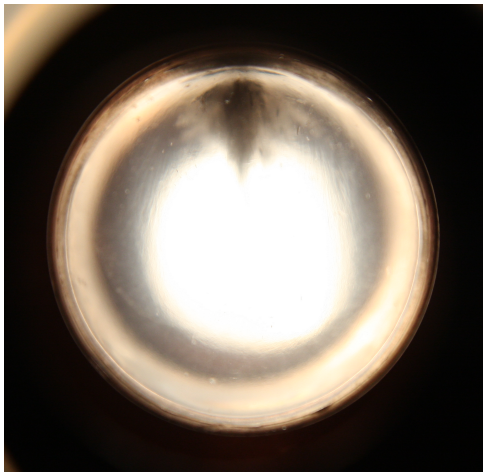

Fig. 2-6 Solid hydrogen by a pressure of 133 mbar after 2.5 hours at 4K. Supplied hydrogen was completely solidified. The dark area on the top is a cracked part of the solid (see the text).

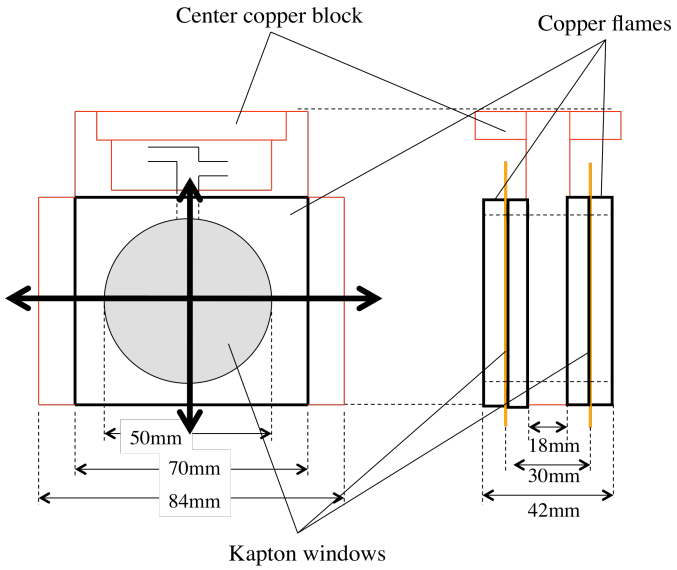

Fig. 3-1 Geometries of the SHT cell used to measure the expansion of the Kapton windows. The target cell (totally 30 mm thickness) consists of three hollowed copper blocks joined into a single square pillar. The Kapton windows were glued on two additional copper flames (6 mm thickness each). The directions for laser scanning (X and Y) are shown by the thick arrows on the front view. Note that the center copper block is larger than other copper blocks and the copper flames.

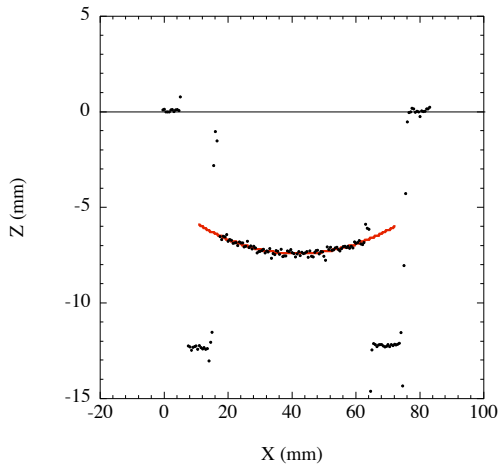

Fig. 3-2 Shape of the Kapton surface on the cell measured by the laser distance meter. X is the horizontal coordinate shown in Fig. 3-1. Z denotes the distance measured by the laser distance meter, where 0mm corresponds to the flat surface of the center copper block. A curvature of between 17 to 67 mm indicates the shape of the swollen Kapton window. The parts ranging 0-17 and 67-84 mm correspond to the surface of the center copper block and the copper flame. We fitted the data points with the second-order polynomial function. The solid line is

the best fitted function.

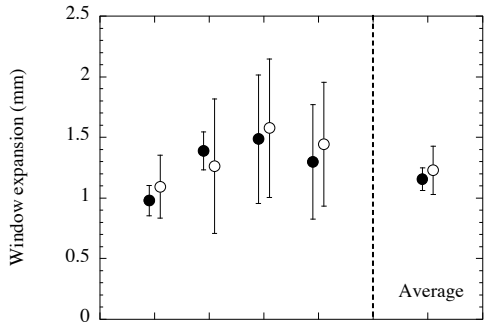

Fig. 3-3 Results of measurements of the surface expansion in the X direction across the center of the Kapton window by the laser distance meter. We measured both ends of the SHT cell 4 times, respectively. The solid and open circles show the different ends of the SHT cell. 'Average' means the surface expansion where the 4 different measurements are averaged.

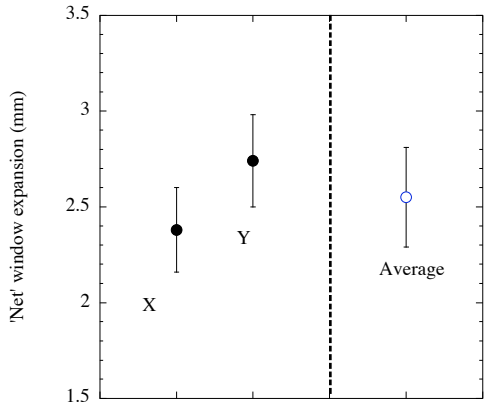

Fig. 3-4 'Total' window expansion measured by the laser distance meter. X and Y mean the horizontal and vertical directions defined in Fig. 3-1, respectively. The data of X was obtained by the sum of averages given in Fig. 3-3.

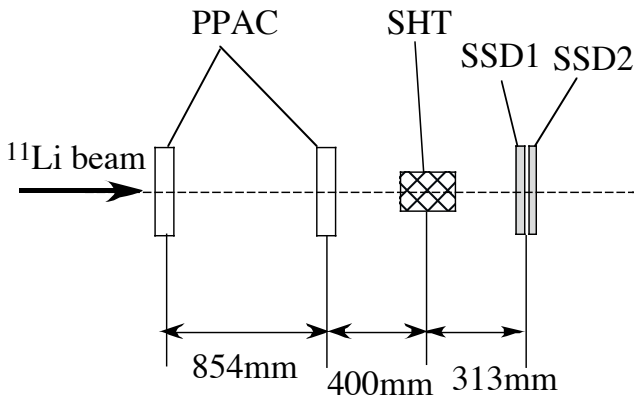

Fig. 3-5 Experimental setup for measurements of the SHT thickness by RI beams. The experiment was carried out at the RIPS facility in RIBF, RIKEN [5].

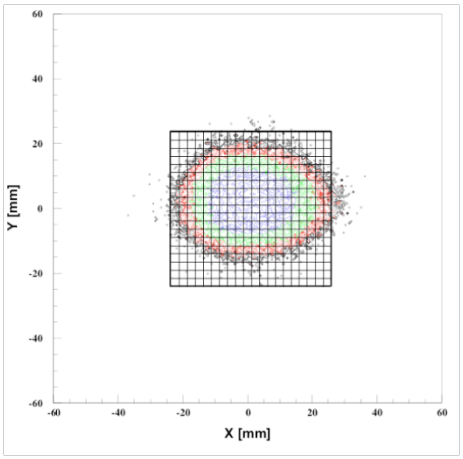

Fig. 3-6 A typical beam-envelope of the ^{11}Li beam on SHT measured by two PPACs located upstream of SHT. X and Y are the horizontal and vertical positions of the ^{11}Li beam, respectively, where 0 mm is the center of the beam. Mesh shows the position gates for ΔE analysis.

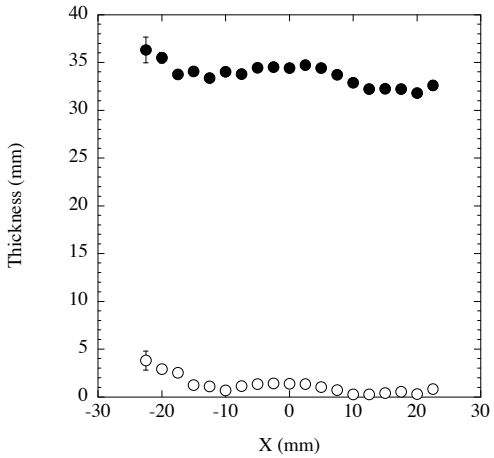

Fig. 3-7 Thickness in the horizontal direction deduced from the measurement by SSD1. Solid and open circles show the thicknesses with and without solid hydrogen, respectively.

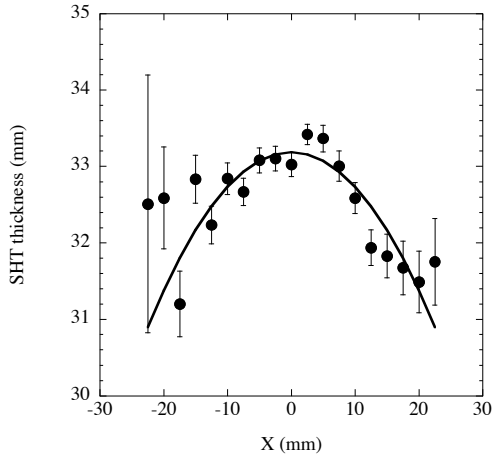

Fig. 3-8 ‘Real’ SHT thickness in the horizontal direction deduced from the measurement by SSD1. The solid line shows the best fitting by a second-order polynomial function.

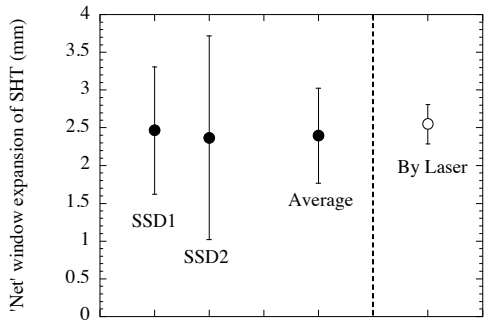

Fig. 3-9 Summary of results for ‘total’ window expansion of SHT. Closed circles show the results deduced from ΔE of ^{11}Li beams for the two SSDs (SSD1 and SSD2). The open circle shows the result measured by the laser distance meter. The data point is the same as ‘Average’ in Fig. 3-4.